Journal of Catalysis **209,** 515–527 (2002)
doi:10.1006/jcat.2002.3649

Spectroscopic Analysis of Au–V-Based Catalysts and Their Activity in the Catalytic Removal of Diesel Soot Particulates

Jeroen Van Craenenbroeck,* Donka Andreeva,† Tatyana Tabakova,† Kristof Van Werde,‡ Jules Mullens,‡ and Francis Verpoort*,[1]

*Department of Physical and Inorganic Chemistry, Ghent University, Krijgslaan 281 (S3), 9000 Ghent, Belgium; †Institute of Catalysis, Bulgarian Academy of Sciences, Academy G, Bonchev Street, bl. 11, 1113 Sofia, Bulgaria; and ‡Laboratory of Inorganic and Physical Chemistry, Limburgs Universitair Centrum, Diepenbeek, Belgium

Received February 4, 2002; revised April 15, 2002; accepted April 17, 2002

Diesel soot oxidation over Au–VO_x/TiO_2 and Au–VO_x/ZrO_2 catalytic systems with different vanadia loadings were studied. The heavy-duty diesel soot was preliminarily analyzed. The composition of the catalysts was investigated by means of FT–Raman. Their activity toward the oxidation of diesel soot was assessed by thermogravimetrical analysis. The combustion onset temperature and the combustion peak maximum can be lowered to 361 and 419°C, respectively. Reaction rates R at certain temperature T_r are calculated out of the first derivative from the mass loss in function of temperature (TGA plot). The results of the activity tests indicate a synergistic effect between Au nanoparticles and vanadia when VO_x presents as a monolayer on the support. Catalysts with higher V loadings show a higher activity but no synergistic effects between Au and V could be observed.

Key Words: **soot oxidation; gold nanoparticles; Raman; TGA–MS; heterogeneous catalysis.**

1. INTRODUCTION

Diesel emissions are known to contain components hazardous to the environment. Soot particulates and nitrogen oxides are the most harmful components in diesel exhaust (1–3). One can easily reduce NO_x components by modifications and/or adjustment of the engine and can apply a suitable after-treatment system to eliminate the second component (3).

Diesel soot particulates are defined by the U.S. environmental Protection Agency as "all compounds collected on a pre-conditioned filter in diesel exhaust gases at a maximum temperature of 52°C." Today, diesel engine modifications and adjustments cause a bimodal size distribution in particulate emissions, which include small nuclei mode particles and larger accumulation mode particles. Most diesel particle mass is contained in the accumulation mode but most of the particle number can be found in the nuclei mode. One assumes that these nanoparticles, which are thought to be the most harmful since they can penetrate deep into the lungs, are condensates of hydrocarbons, water, and sulfuric acid (4).

A suitable after-treatment system to eliminate the soot particulates needs to meet two requirements: acceptable activity in the temperature window and a high resistance to sulfur deactivation. Many catalytic systems developed so far are sensitive to sulfur and are irreversibly deactivated by sulfur compounds in diesel exhaust, even at low concentrations (5, 6). Sulfur compounds are oxidized in the engine chamber mainly to SO_2 (>95%). A minor amount of SO_3 (<5%) reacts with water vapor or metal oxides to form sulfuric acid or metal sulfates, respectively. New EURO legislation concerning the emissions of pollutants by passenger cars requests a large reduction in sulfur concentration to 50 ppm in diesel fuel by the end of 2005 (4, 7, 8). From this date on, sulfur-free fuels (<10 ppm) will be introduced in every Member State and will be a requirement by the end of 2011. These sulfur-free fuels are being proposed primarily to enable advanced emission control technologies that are sulfur intolerant.

Typically, a soot particle consists of a carbon nucleus, contaminated with metal compounds, with a number of different hydrocarbons, the so-called SOF (soluble organic fraction), and sulfates adsorbed on their surface (3, 4). The most elegant way perhaps to eliminate soot particulates from diesel exhaust is to apply an appropriate filter material coated with catalytic material with strong oxidation properties. In the past decades a lot of effort has gone into this field (8–19). Research has been focused on metal compounds with strong redox properties. Recently gold nanoparticles on a surface were found to be very active in different oxidation reactions at low temperatures. CO is easily oxidized in this way even at room temperature (20–22). This high activity has also been found for other reactions, such as the complete oxidation of benzene (23), the water–gas shift reaction (24, 25), and the reduction of NO (26).

In this study, we report on the combination of the oxidation properties of the gold nanoparticles with the redox

[1] To whom correspondence should be addressed. Fax: (+32)09/264.49.83. E-mail: francis.verpoort@rug.ac.be.

0021-9517/02 $35.00

properties of vanadia. Au-based, V-based, and Au–V-based catalysts have been synthesized and tested for the oxidation of diesel soot and have been checked for synergistic effects.

2. EXPERIMENTAL

2.1. Synthesis

All the samples were synthesized in an automated laboratory reactor "CONTALAB" (Contraves, Switzerland), using a deposition–precipitation method, with complete control of all parameters of preparation: pH (7.0), temperature (60°C), reactants feed flow rates, stirrer speed (250 rpm), and so forth. The preparation involved the deposition of gold hydroxide onto the support through the chemical interaction of $HAuCl_4 \cdot 3H_2O$ and Na_2CO_3 in aqueous solution. Supports were TiO_2 (anatase) prepared by hydrolysis of $TiCl_4$ with ammonia at pH 9.0 at low temperature and commercial ZrO_2. After aging for 1 h at 60°C the precipitates were filtered and carefully washed until there was an absence of Cl^- ions. The samples contained 3 wt% Au. The V_2O_5-containing samples were prepared by impregnation with different amounts of $(NH_4)_2[VO(C_2O_4)_2]$. The samples were dried under vacuum at 80°C, calcined in air at 400°C for 2 h, and stored in an exicator. All chemicals used were "analytical grade." Composition of the five zirconia-based samples and seven titania-based samples synthesized is summarized in Table 1.

2.2. Analysis

2.2.1. Soot. To have an idea about the composition of the soot, preliminary analysis of the heavy-duty diesel soot particulates was carried out by semiquantitative energy dispersive X-ray analysis (EDAX) (Philips 5010) with a system resolution of 63 eV. All elements were scanned, normalized, and quantified by the ZAF method (seven iterations).

TABLE 1

Composition of the Different Catalysts Synthesized

Sample	Support	V (%)	Au (%)
AT	TiO_2	—	3
4VT	TiO_2	4	—
8VT	TiO_2	8	—
12VT	TiO_2	12	—
4VAT	TiO_2	4	3
8VAT	TiO_2	8	3
12VAT	TiO_2	12	3
AZ	ZrO_2	—	3
2VZ	ZrO_2	2	—
4VZ	ZrO_2	4	—
2VAZ	ZrO_2	2	3
4VAZ	ZrO_2	4	3

Note. V loadings were calculated as the percentage of V_2O_5 and Au loadings as the percentage of Au.

Specific surface area measurements (BET) were performed at liquid nitrogen temperature in a Micromeritics Gemini apparatus. TGA analysis of the soot was carried in a Stanton Redcroft STA1500 TGA/DTA (simultaneous thermal analysis) at a heating rate of 5°C/min under air and under inert atmosphere (N_2). The soluble organic fraction (SOF) of the soot was extracted with THF three times and analyzed by means of FT-IR spectroscopy on a Mattson Research Series spectrometer.

2.2.2. Catalyst. The BET specific surface area analysis of the untreated support materials was performed at liquid nitrogen temperature in a Micromeritics Gemini apparatus.

The vanadates and the compounds formed by calcination were analyzed by means of FT–Raman. Analysis of the powdered samples was performed on a Bruker FT–Raman/IR spectrometer with a Nd–YAG laser ($\lambda = 1064$ nm) and a nitrogen-cooled Ge detector. The setting parameters are the laser power and the number of scans. Applying a nonfocused 250-mW laser beam, 2000 scans, and a resolution of 3 cm^{-1} showed clear spectra for zirconia samples. The titania samples required a nonfocused 300-mW laser beam to obtain useful spectra. All spectra were vector normalized.

2.3. Catalytic Activity Tests

The different samples were prepared by mixing the catalyst powder and the soot in a catalystsoot weight ratio of 2 : 1 with a spatula ("loose" contact) without any preceding treatment.

TGA–MS experiments were performed with a TGA 951–2000 apparatus from TA instruments coupled to a quadrupole mass spectrometer (Model Thermolab of VG Fisons Instruments), using a flexible heated silica-lined steel capillary and a molecular leak coupled to evolved gas analysis (TGA–EGA). The scanning range of the MS was set from mass 0 to 50. In all experiments a heating rate of 10°C/min was applied.

Differential thermal analysis (DTA) was carried out in dry air on a DTA 1600–2000 from TA instruments. For DTA a heating rate of 10°C/min was considered.

3. RESULTS AND DISCUSSION

3.1. Analysis

3.1.1 Soot. Semiquantitative EDAX showed the presence of 1.6 wt% S and a minor amount of the metals Zn, Fe, Ca, and Cu (<1 wt%) originating from the fuel, lubricant, or the engine. To determine the amount of volatile compounds adsorbed on the carbon surface a TGA run was carried out under nitrogen atmosphere. After heating to 300°C the soot mass was reduced to 55 wt% of its original mass and to 49% when 600°C was reached, meaning that half of the soot mass can be considered volatile. This is confirmed by the accompanied DTA plot, which clearly shows

the endothermic nature (evaporation) of the physical process. Two major endothermic bands corresponding with the largest mass loss are found: a large band at 60°C and a minor band around 180°C. The first band can be attributed mainly to the evaporation of adsorbed H_2O. At higher temperatures HC and sulfur compounds desorb from the surface.

FT-IR analysis of the SOF after extraction with THF shows the presence of aliphatic and aromatic compounds. At low frequencies (650–450 cm^{-1}) small bands can be found that are attributable to organic sulfur compounds. Performing a TGA/DTA run in air of the extracted soot showed no mass loss at low temperatures and no accompanying endothermic DTA bands could be found. Specific surface area of the fresh and extracted soot measures were 26 and 68 m^2/g, respectively, as determined by BET analysis.

In air the carbon nucleus starts to oxidize around 505°C, with the highest oxidation rate at 532°C. At 600°C the soot mass has been decreased to 7 wt% of its original mass. The rest of the fraction, the so-called ashes, mainly consists of inorganic oxides.

3.1.2. Catalyst. TEM analysis of the catalysts revealed the presence of well-dispersed small gold nanoparticles in a range of 1.5–5 nm, with an average diameter of 2 nm.

BET analysis of both supporting materials applied in this study showed a specific surface area of 94 and 19 m^2/g for TiO_2 and ZrO_2, respectively.

FT–Raman spectroscopy gave additional information about the surface composition of the catalyst. Spectra of the untreated support materials showed strong bands below 600 cm^{-1}. The frequency range of interest is situated between 1100 and 800 cm^{-1}, so the bands from the support do not interfere with the bands originating from the catalytic surface material. Supported vanadium has been a subject of considerable interest because of its wide applications as a catalyst in many reactions and because it represents a model for the analysis of interactions at the oxide/surface interface (27–31). The formation of crystalline bulk V_2O_5 starts after the surface has been covered with a monolayer of different poly- and monovanadates species. These two-dimensional overlayers of surface vanadium oxide species are thought to be the active redox sites, where crystalline bulk vanadium oxide is supposed to be less active in catalytic reactions. These observations have provided motivation for investigations into the structure and distribution of the dispersed VO_x species and their influence on the catalytic properties of these materials. Several authors (29, 31) agree that at low V loadings fourfold coordinated monovanadates species are present on the surface, characterized by a band at 1030 cm^{-1}, indicative for a strong V=O bond. At higher V loadings broad V=O stretching bands appear in the lower frequency range (1000–900 cm^{-1}), attributable to the V=O stretch of polymeric vanadium species or V_xO_y "clusters" formed on the surface. Below 900 cm^{-1} bands from ν(V–O–V) appear. Further increase in V loading results in the formation of V_2O_5 crystallites after full coverage of the surface with a monolayer with a typical band at 997 cm^{-1}.

It should be noted that vector normalization was necessary to obtain useful spectra since a small amount of the catalyst was present only on the surface. Therefore quantitative derivations need to be done with care.

For the titania-based samples, as shown in Figs. 1a and 1b, different vanadium compounds can be found depending on the V loading. 4VT shows a small band at 1030 cm^{-1} originating from the V=O stretch of monovanadyls and two broad bands below 1000 cm^{-1} are attributable to the internal (974 cm^{-1}) and terminal (945 cm^{-1}) V=O stretching vibrations of the polyvanadates. The bands at 881 and 847 cm^{-1} are indicative for the V–O–V stretch vibration. The bands of polymeric species tend to shift to higher frequencies when a higher amount vanadium is applied: from

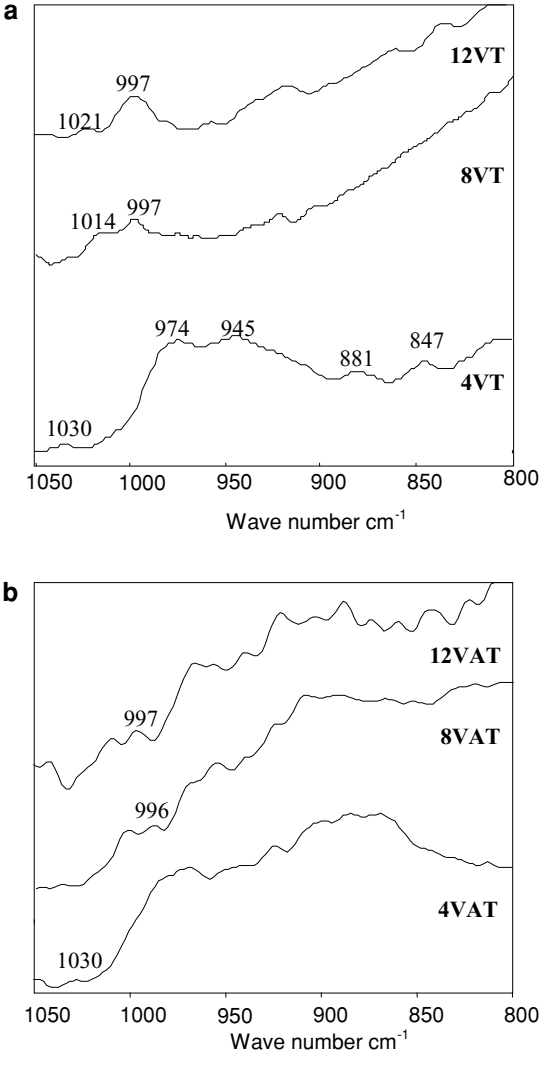

FIG. 1. Raman spectra of the VT samples (a) and the VAT samples (b).

974 to 1014 and 1021 cm^{-1} and from 945 to 997 cm^{-1}, a shift of approximately 50 cm^{-1}, for 8VT and 12VT, respectively. As the number of vanadium centers in the polyvanadates increases, the number of terminal V=O groups per vanadium decreases to accommodate V–O–V linkages. This results in a shift in the frequency of the remaining bonds from ~950 to ~1000 cm^{-1} (27). The V–O–V band also shifts about 50 cm^{-1}, from 881 to 920–930 cm^{-1}. It is unlikely that the band at 997 cm^{-1} in 8VT and 12VT originates only from the terminal polymeric V=O stretch since this frequency coincides with the frequency typical for crystalline V_2O_5. The formation of crystalline V_2O_5 on TiO_2 starts to form at 6 wt% (27). The band found at 997 cm^{-1} at higher V loadings (8 and 12 wt%) is therefore probably a superposition of two bands. Another indication is the relative intensities of the bands of the internal V=O and terminal V=O. One expects a relative decrease in the intensity of the terminal V=O-band at 997 cm^{-1} for 8VT and 12VT and a relative increase in the internal V=O band around 1020 cm^{-1}, as well as an increase in the V–O–V band at higher V loading. But looking at the relative intensities of these two bands and compared to the bands at 974 and 945 cm^{-1} in the 4VT sample it is obvious that the band at 997 cm^{-1} is a superposition of two bands. For 12VT a large amount of crystalline V_2O_5 is formed and polymeric species are present in an inferior amount. No evidence for the existence of monovanadyls could be found at high V-loadings.

It should be pointed out that adding 3 wt% Au (Fig. 1b) onto the surface resulted in spectra with a higher noise level and less resolution. Nevertheless, gold particles seem to favor the formation of polyvanadates instead of V_2O_5 crystallites at high V loadings (23a). Besides a relative increase in the band below 900 cm^{-1} from the V–O–V stretch no significant changes are observed in the spectrum of 4VAT. A small band at 1030 cm^{-1} from the monovanadyls and broad bands below 1000 cm^{-1} from the polyvanadates appear in both spectra. Remarkable changes have been observed when Au is present at higher V loadings. The band due to crystalline V_2O_5 diminishes dramatically. In contrast, the polyvanadates are highly represented, looking at the bands in the range below 1000 cm^{-1}. Apparently Au particles seem to favor the linkage of V–O–V bonds over the formation of V_2O_5 crystallites. The reason for this influence is still unclear since Au is not spread out on the surface but is concentrated in local particles, implying a very local influence on the kind of vanadia species formed. However, these species can be thought to be vanadia clusters originating from V_2O_5 crystallites rather than vanadia chains.

Applying only 3 wt% Au on the surface showed no specific signals, only those originating from the support material.

For the zirconia-based samples (Figs. 2a and 2b) a sharp band at 997 cm^{-1} attributable to the presence of V_2O_5 crystallites in all samples can be found, even at low V loadings.

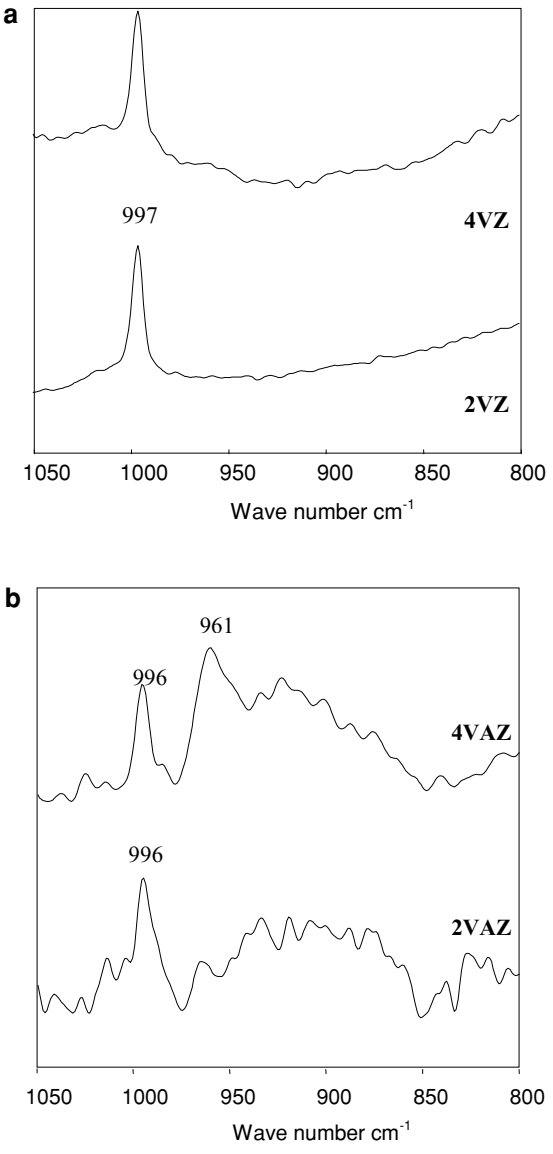

FIG. 2. Raman spectra of the VZ samples (a) and the VAZ samples (b).

This is in agreement not only with the BET analysis, which showed a specific surface area which is four times smaller for ZrO_2 than for TiO_2, but also with the nature of the support (23a). The existence of other vanadia species is thought to be inferior to the presence of V_2O_5 crystallites since the bands attributable to the respective species disappear in the noise level. Applying Au causes the same trend as with the titania samples. The formation of V–O–V bonds seems to be promoted instead of V_2O_5 crystallites, looking at the spectra of 2VZ, 4VZ and 2VAZ, 4VAZ, although an amount of crystalline V_2O_5 is still present, as confirmed by the band at 996 cm^{-1}. This promotional formation is less distinct for the zirconia samples than for the titania samples.

3.2. Catalytic Activity Tests

All TGA plots of the different samples showed a mass reduction of 30% (±4%), consistent with the amount of soot applied in the catalyst/soot mixtures and with the uncatalyzed soot oxidation plot, implying a complete oxidation of the soot particulates when 600°C is reached. The reaction products are detected by qualitative mass spectrometry (MS). From the MS plot one can follow the desorption and formation processes in a qualitative way. Since all MS spectra are similar, only one is shown in Fig. 3. The large increase in the signal at the channel with a m/e of 44 (CO_2^+) in the higher temperature range is due to CO_2 formed as a major oxidation product from the carbon nucleus. At the same time the O_2 signal (m/e 32) dramatically decreases. At this point the largest mass loss occurs, as can be seen in the corresponding TGA plots. In the lower temperature range a signal at m/e 18 (H_2O^+) is found that is attributable to the evaporation of adsorbed H_2O (<100°C). SO_2 formed from decomposition of sulfur compounds is detected as a SO^+ fragment (m/e 48) and not as SO_2^+ (m/e 64) since the scanning range was set up to m/e 50.

A parallel test run was performed by DTA analysis. A strong exothermic DTA signal in the same temperature range as the CO_2 detection and the largest mass loss can be found, according to MS and TGA results, respectively. A broad endothermic band has been observed in the lower temperature range due to evaporation processes, as mentioned above. Nevertheless one did not use the DTA plots for the derivation of activity parameters since the catalyst/soot sample is liable to a very local exothermic process, especially during ignition of the soot. Therefore derivations could be deceptive, given that, according to DTA, the largest mass loss from TGA does not correspond to the largest heat production. A direct measure for activity is the reaction rate, and thus in this study the mass loss of reactant (soot) per time unit and not the heat production per time unit.

The following parameters have been derived. The reaction rate R at a certain temperature T_r from the first derivative of the TGA plot. Another parameter, which is very characteristic for a catalytic system, is the ignition temperature, T_{ign}, the temperature at which the oxidation of the carbon nucleus starts. Unfortunately an exact derivation of this parameter is difficult, if not impossible, from this data and has not been mentioned for other systems by other researchers. Since MS is more sensitive than TGA it should be more correct to derive the ignition of the nucleus from the CO_2 formation or O_2 consumption out of MS data. Nevertheless T_{ign} has been derived out of the derivative of the TGA plot because the CO_2 signal does not reflect the overall mass loss. Besides, the derived T_{ign} makes it possible to compare ignition with the further oxidation process since they are obtained from the same plot.

Generally, the Au–V catalytic systems enhance the oxidation of the soot and decrease the oxidation process temperatures T_r and T_{ign} 100°C or more, typically to the desired temperature range of 300–400°C.

In Figs. 4a–4f the first derivative of the TGA plot and the CO_2 signal are shown for the different titania samples. The plots are given versus time and therefore each figure

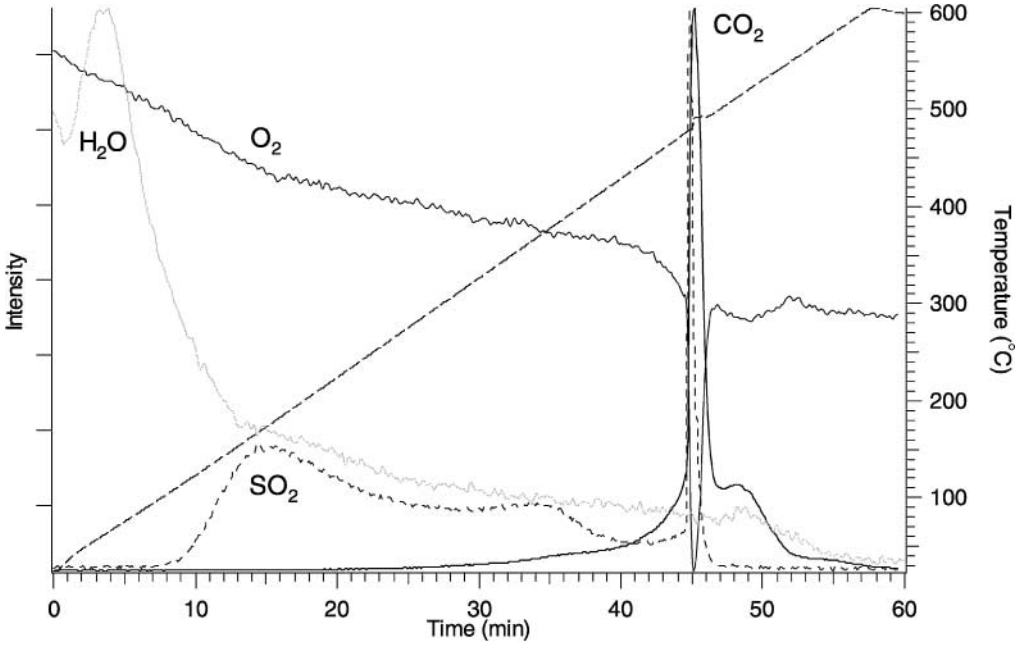

FIG. 3. MS spectrum of AT.

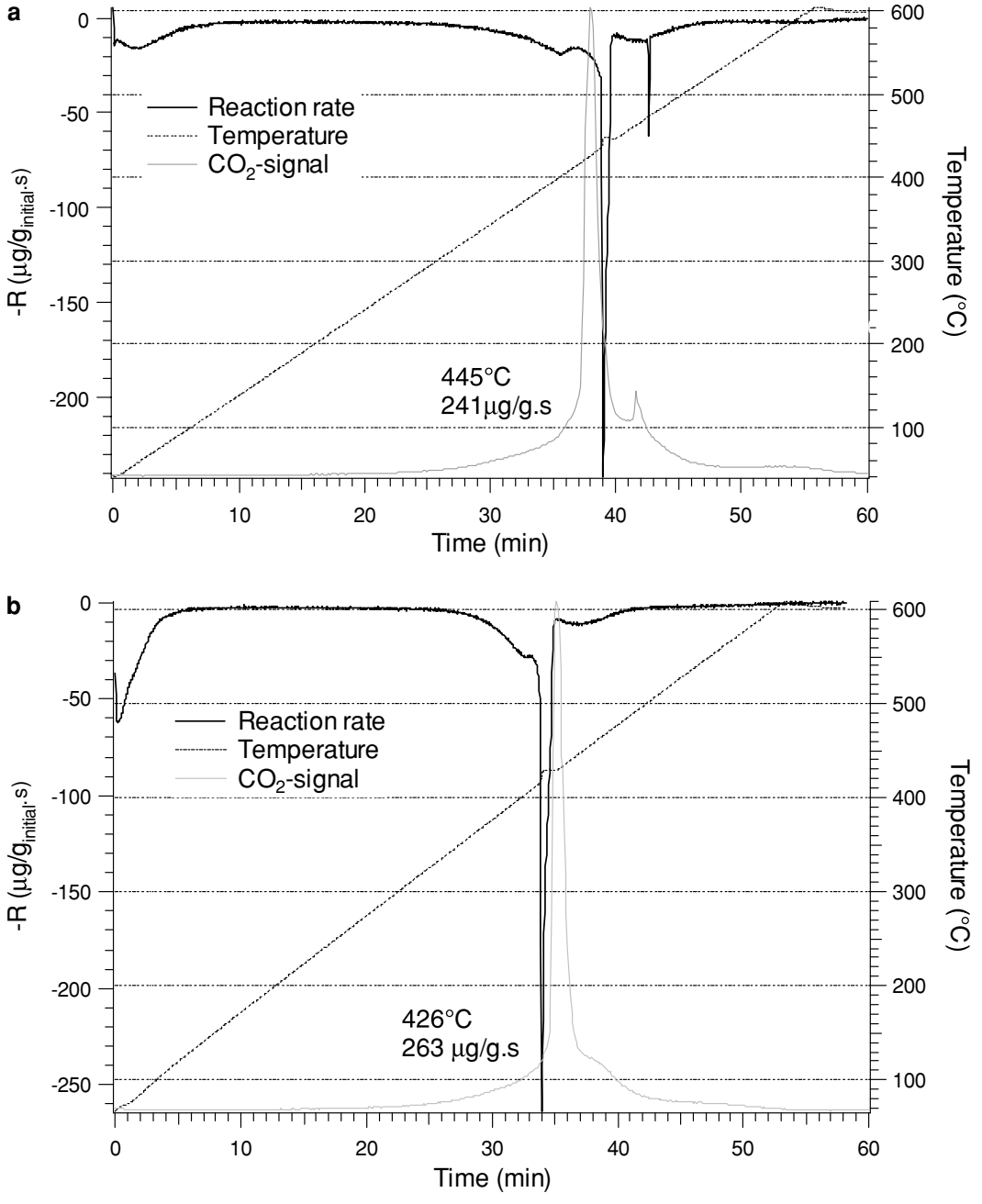

FIG. 4. Reaction rate R and CO_2 signal vs time of 4VT (a), 8VT (b), 12VT (c), 4VAT (d), 8VAT (e), and 12VAT (f).

contains a temperature line as well. For the zirconia samples the respective plots are not given but the parameters derived here are shown in Tables 2–5. In Table 2 the temperature when a maximum in reaction rate R ($\mu g \cdot g^{-1} \cdot s^{-1}$), T_{max}, has been reached is mentioned. This table includes also an uncatalyzed test run of soot. The support materials do not exhibit significant activity and are therefore not mentioned. The value of the maximum in reaction rate is not a parameter for comparing the activity of the different samples since they occur at different temperatures.

To have a clearer view of the activity it is interesting to look at T_r for a given value of R or to look at R for a given T_r. Therefore T_r when a reaction rate of 150 $\mu g \cdot g_{init}^{-1} \cdot s^{-1}$ was reached and R at 370, 390, and 410°C for the different catalysts are summarized in Tables 3 and 4, respectively. The zirconia samples as well as the vanadia-free samples AT and AZ are not mentioned in Table 4 because they showed only very low activity at the given temperatures. Uncatalyzed soot is not mentioned in either table since R is very low and never reached a value of 150 $\mu g \cdot g_{init}^{-1} \cdot s^{-1}$. The experimental

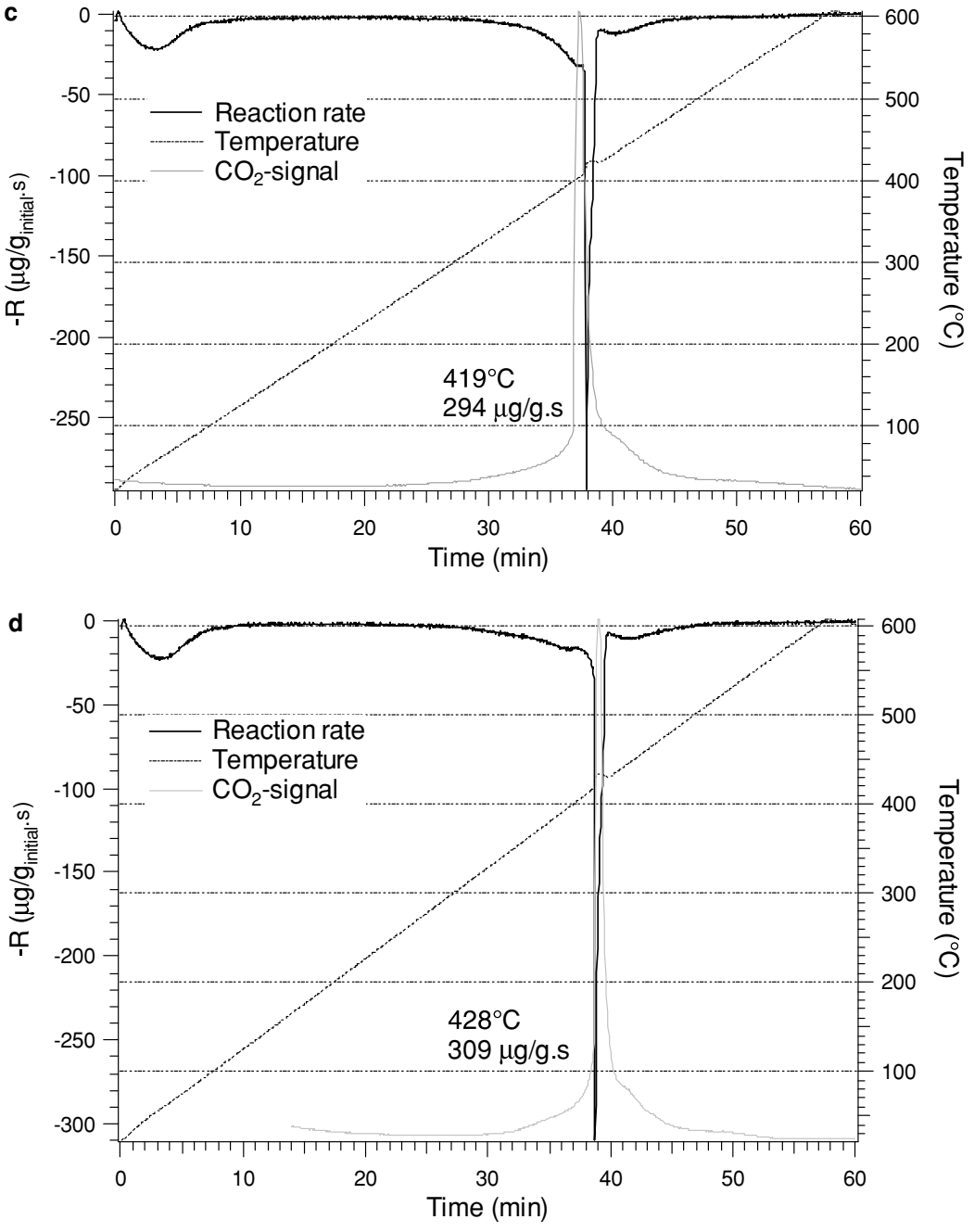

FIG. 4—*Continued*

error in the determination of T_r, as shown in Table 3 and Fig. 5, is smaller than 1°C in this temperature range, the interval between two measured points in the reaction rate. One should interpret the values of the reaction rates shown in Table 4 in a relative rather than an absolute way since the exact value of the parameter often was between two measured points, although they are in the same order of magnitude as other catalysts studied (3).

In Fig. 5 T_r for the titania- (Fig. 5a) and the zirconia (Fig. 5b)-based samples with and without Au, as shown in Table 3 is plotted versus V loading.

From these data one can see that for the titania-based samples T_r decreases as vanadium loading increases (4VT, 8VT, and 12VT). Different authors claim that the catalytic sites with highest activity are monovanadyl (29, 31) and polyvanadate sites (32), implying that the highest activity occurs with a monolayer on the surface (23a, 32). According to our Raman results monovanadyls are present only at low V loadings (4VT), although the activity increases with higher V loadings. The reason for this can be found in the fact that for solid–solid reactions the contact area between the reactants, i.e., between catalytic sites and the

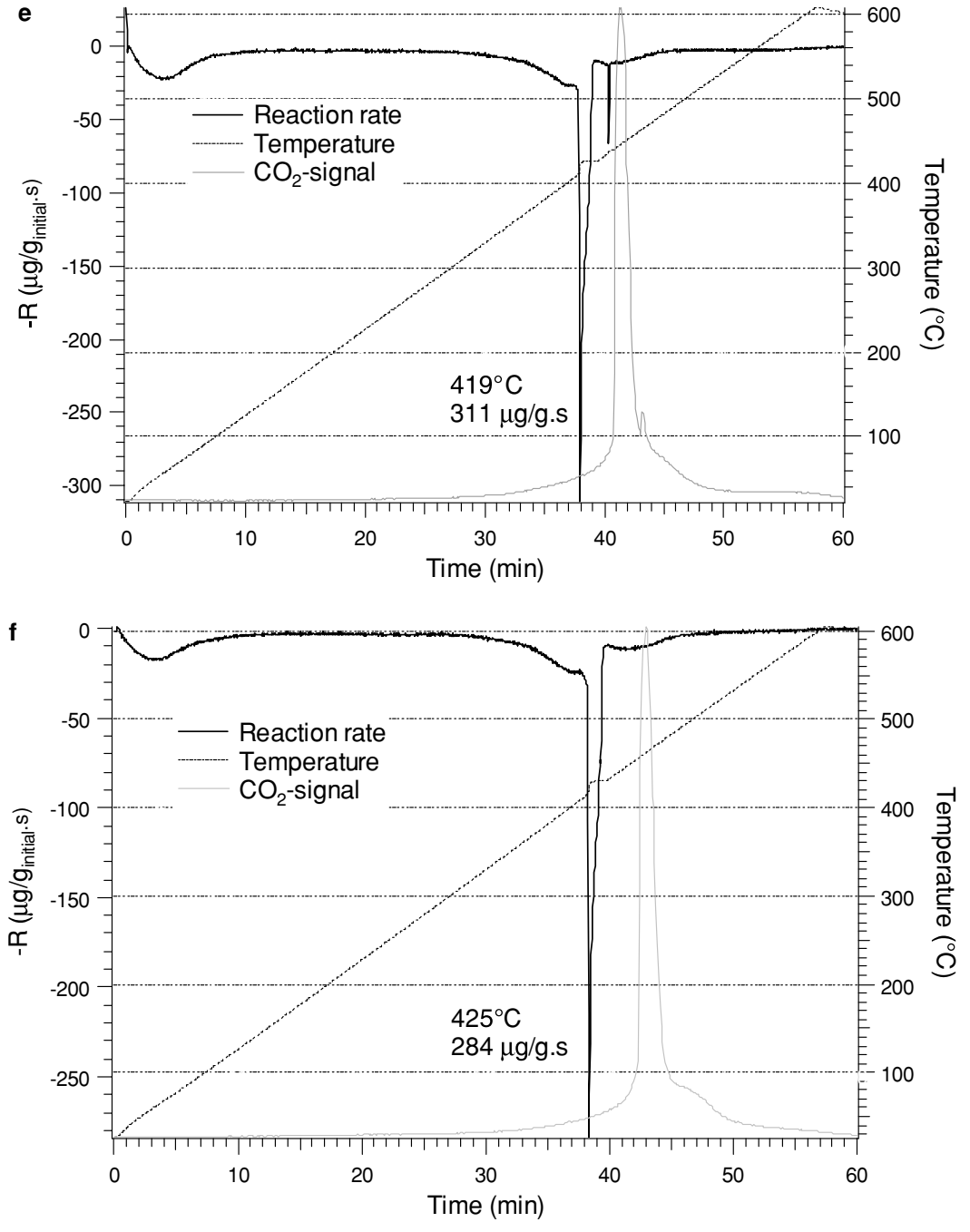

FIG. 4—*Continued*

soot, is of great importance (3, 33). Since the number of contact points is proportional to the catalyst concentration one can expect an increase in activity with higher surface loadings. In this case it even seems that this contact area is a rate-determining factor because the difference in inherent activity of the several species is of less importance than the contact between soot and catalyst, i.e., the concentration of catalytic sites in contact with the soot regardless their nature. Another argument for this is the Tammann temperature of the bulk V_2O_5, defined as the temperature at which the material presents a certain surface mobility and which is generally situated at around 1/2 the melting point of the metal oxide (31). The Tammann temperature of V_2O_5 ($T_m = 690°C$) lies within the activity window of the catalysts. Under these circumstances the catalyst is able to increase the contact between soot and catalyst because of its

TABLE 2

Temperature (T_{max}) at Highest Reaction Rate (R) for the Different Samples under Air at 10°C/min

Sample	T_{max} (°C)	Sample	T_{max} (°C)
Soot	532	AT	490
		AZ	511
4VT	445	4VAT	428
8VT	426	8VAT	419
12VT	419	12VAT	425
2VZ	475	2VAZ	479
4VZ	454	4VAZ	478

"wetting" capability. Catalysts with low melting points for this reaction have been studied by Moulijn and co-workers and shown to be very promising (34, 35).

Adding 3 wt% Au seems to induce promotional effects at low V loadings, looking at 4VT and 4VAT. It is known that Au nanoparticles are very active oxidation catalysts for gaseous reactions at low temperatures. Their role herein consists of adsorbing molecular oxygen and forming peroxo–Au species in this way (36). In this reaction the nanoparticles show little activity (AT) but when other catalytic redox sites, such as vanadia, are present Au seems to operate as an oxygen donor to the catalytic mono- and

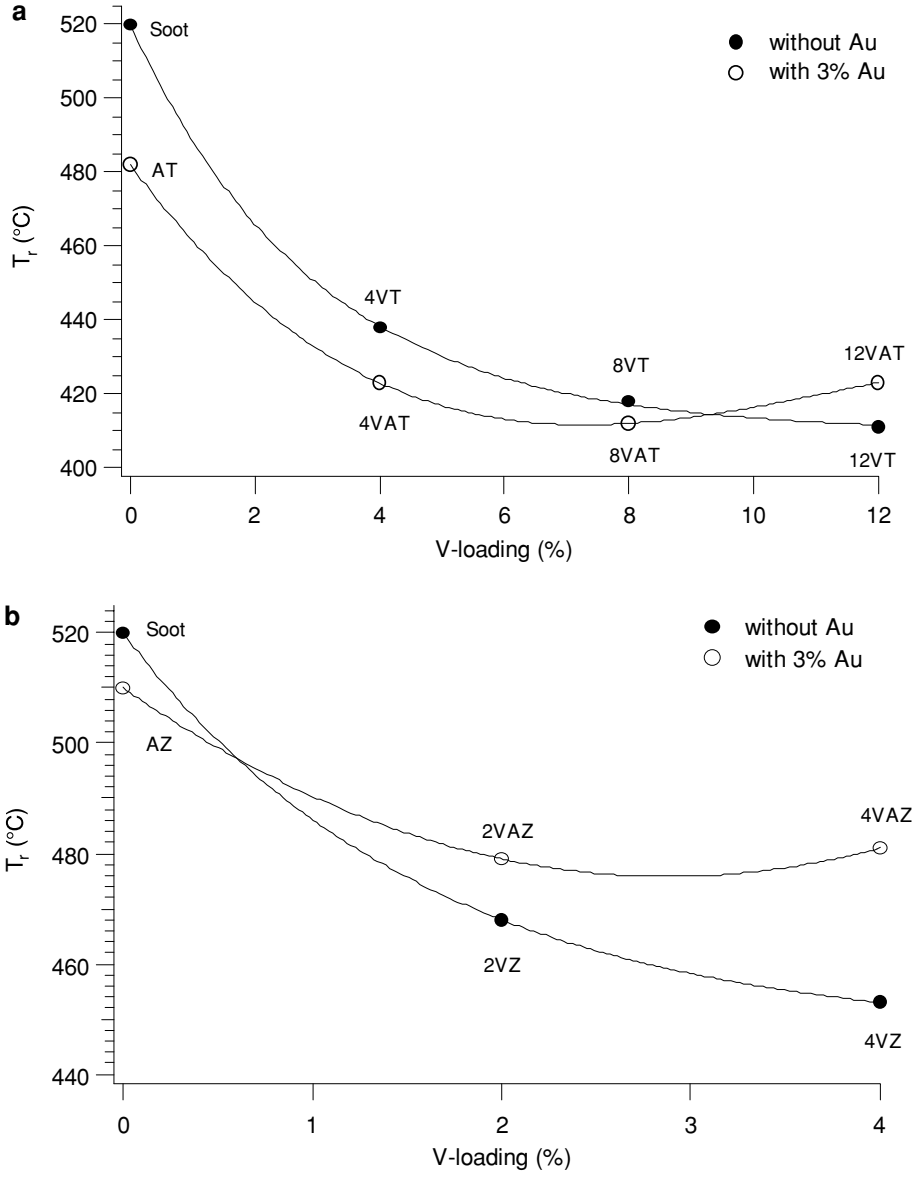

FIG. 5. V-loading dependence of T_r at $R = 150\ \mu g \cdot g_{init}^{-1} \cdot s^{-1}$ for the titania samples (a) and the zirconia samples (b).

TABLE 3

Temperature (T_r) When a Reaction Rate of 150 $\mu g \cdot g_{init}^{-1} \cdot s$ Has Been Reached under Air at 10°C/min for the Different Samples

Sample	T_r	Sample	T_r
Soot	520	AZ	510
		AT	482
4VT	438	4VAT	423
8VT	418	8VAT	412
12VT	411	12VAT	423
2VZ	468	2VAZ	479
4VZ	453	4VAZ	481

polyvanadia sites (Au–V sites), looking at 4VT–4VAT. This effect diminishes at higher V loadings, looking at 8VAT and 12VAT. At 12% V the addition of Au even results in a small inhibitional effect. The lack of promotional effects is probably due to the coverage of gold nanoparticles by vanadia species and the promotional adsorption sites are inhibited in this way. It is unlikely that the small difference between 8VT–8VAT and 12VT–12VAT is due to experimental errors since T_r can be determined to within an error of ±1°C within this temperature range. For an explanation one has to look at the nature of the vanadia species, according to the Raman results, where Au seems to promote the formation of polyvanadia species instead of V_2O_5 crystallites. These polyvanadates are thought to be clusters such as $(V_{10}O_{28})^{2-}$ or $(HV_2O_7)^{3-}$ (31), originating from distortion of the vanadia microcrystallite structure rather than chains. A driving force for their formation out of crystallites might be again the oxygen donor property of the Au nanoparticles since vanadia clusters tend to contain more oxygen atoms per vanadia atom than does crystalline V_2O_5. By this formation the wetting properties of the catalysts diminish since the low-temperature-melting crystallites disappear. The resulting activity of 8VAT and 12VAT is a superposition of two opposing effects. First there is the promotional effect of gold nanoparticles for the vanadia species (mono and poly) resulting in higher activity. The diminishing of the wetting properties by disappearance of V_2O_5 crystallites results in a decrease in activity. The overall result shows again the great importance of the contact between soot and catalyst, looking at 12VAT, where most of the crystalline V_2O_5 has disappeared, according our Raman data, although more active Au–V sites are created. For 8VT the diminishing of the wetting property by the decrease of crystalline V_2O_5 present on the surface does not compete with the formation of more-active sites formed in this way and the amount of polyvanadate sites already present on the surface, resulting in a small promotional effect.

TABLE 4

Reaction Rate (R) at Different Temperatures (370, 390, and 410°C) under Air at 10°C/min for the Titania Samples

	T_r (°C)		
Sample	370	390	410
4VT	10	15	17
8VT	9	15	17
12VT	11	22	104
4VAT	12	16	19
8VAT	12	22	31
12VAT	12	20	24

The inhibitional effect is even more clear for the zirconia-based samples, looking at 2VZ–2VAZ and 4VZ–4VAZ in Table 1. Gold-based samples show a lower activity than gold-free samples. According to our BET results showing a specific surface area of 19 m^2/g, four times less than that of titania, 94 m^2/g, one expects a full coverage of the surface and the appearance of crystalline V_2O_5 even at low loadings. This is confirmed by Raman analysis showing clear evidence for the presence of V_2O_5 crystallites.

One should expect high activity for 4VZ according to the reasoning above since V_2O_5 crystallites are the major compound present, looking at the Raman spectra. Nevertheless the 4VZ sample shows very little activity compared to the 4VT sample where the same amount of vanadia is present. It is known that the supporting material may contribute to the total catalytic activity of the system for this reaction (37).

Among the catalysts studied so far the promotional effect is the strongest for 4VAT and its activity competes with 12VT, again showing the importance of contact points between soot and catalyst, in addition to the nature of the site (Fig. 5).

Reaction rates shown in Table 4 are plotted versus V loading in Fig. 6. Looking at the gold-free samples one can clearly see the relation between reaction rate and V loading. The superior activity of the 12VT sample is due to good contact between the soot and the catalyst. Adding gold does not influence the rate greatly except at high V loadings where V_2O_5 is present on the surface. Where the shape of the plots for the gold-free samples shows an exponential correlation, there is a Gaussian correlation when Au is present. This volcano shape with a maximum suggests a superposition of two opposing effects: The good contact between soot and catalytic sites (i.e., the number of sites together with the wetting properties) when high amounts of vanadia are used results in an increase in R, and the diminished promotional effect of Au at higher V loadings results in a decrease in R. The superposition of these effects gives a volcano-shape plot with a maximum. This maximum should be interpreted as a compromise between these two effects rather than an exact physical value. The difference between the exponential behavior and the Gaussian behavior is the strongest at high V loadings. When 12% V is applied, the reaction rate decreases dramatically when Au is present

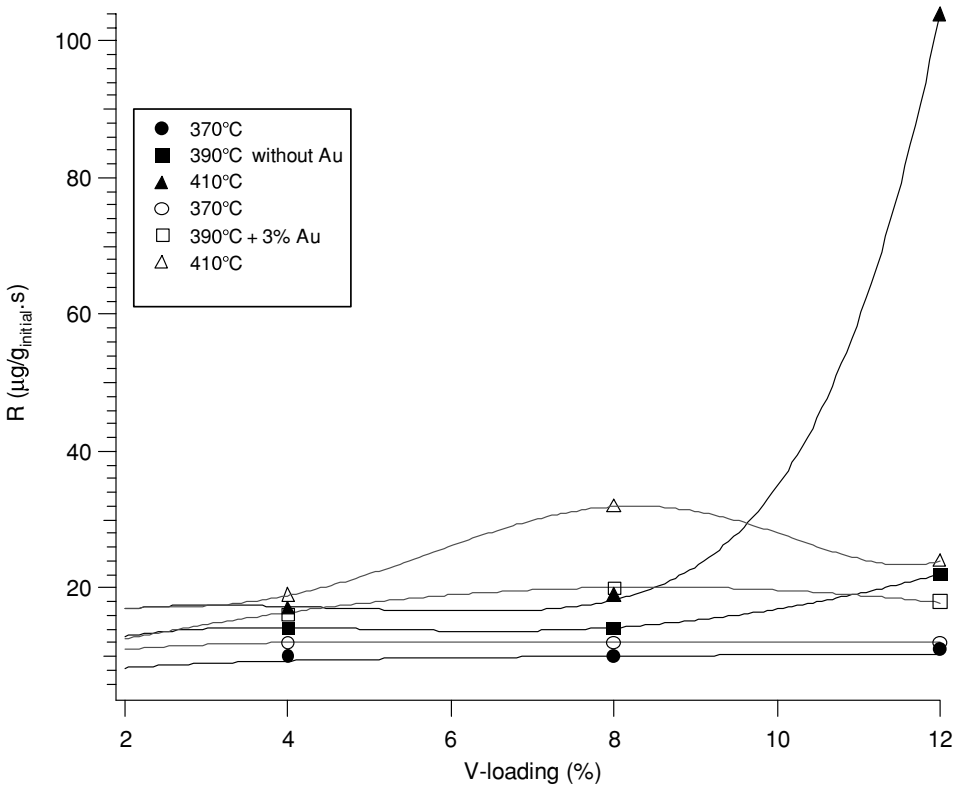

FIG. 6. V-loading dependence of the reaction rate R at different temperatures for the titania samples.

(12VT–12VAT) due to a diminished contact, although sites with higher intrinsic activity are present.

The second parameter, T_{ign}, again derived from derivative TGA data and defined as the starting point at which the carbon nucleus ignites, is more difficult to derive and probably therefore never mentioned by other authors, despite its practical merit. Table 5 contains the T_{ign} for the different samples. These values should be taken with an estimated error of ±5°C. Low values of T_{ign} indicate the presence of very active sites able to lower the activation energy enough. T_{ign} reflects the nature of the active species regardless of the number of those catalytic sites present. Once the ignition takes place, the number of catalytic active sites becomes important.

TABLE 5

Onset Temperature (T_{ign}) under Air at 10°C/min for the Different Samples

Sample	T_{ign} (°C)	Sample	T_{ign} (°C)
Soot	505	AT	471
		AZ	466
4VT	366	4VAT	363
8VT	369	8VAT	361
12VT	367	12VAT	365
2VZ	394	2VAZ	383
4VZ	390	4VAZ	381

All titania (VT and VAT) samples ignite in the same temperature range (360–370°C), although there is a difference in activity between VT and VAT samples at higher temperatures (R and T_r). Adding Au to the VT samples does not change T_{ign} remarkably. This is not the case for the zirconia samples (VZ and VAZ). The relatively higher T_{ign} for the VZ samples is small but significant and can be attributed to the nature of the catalytic active sites. Catalytic sites with lower intrinsic activity tend to form when zirconia is used as support. Looking at our Raman data, sites with a crystalline nature are formed. Adding gold to the system lowers the T_{ign} of the zirconia samples 10°C but not for the titania samples. Herein one can clearly see the promotional effects of gold. For the zirconia samples V_2O_5 crystallites are the main species on the surface. Adding gold promotes the formation of more-active sites like polyvanadates, instead of crystallites, with a higher intrinsic activity able to lower T_{ign}. This is not the case for the titania samples, where different kinds of species are present even without Au added. Adding gold to the VT samples does not provide even-more-active sites, only a larger number of intrinsic very active sites. In this way the role of the gold nanoparticles is reduced to being a promoting oxygen donor once the vanadia site becomes active (T_{ign}).

Au is able to create very active catalytic sites out of crystallites able to lower T_{ign} to the desired temperature range. Once the ignition has taken place, the number of contact points becomes important and determines the further oxidation process. The difference between T_{ign} from Table 5 and T_r from Table 3 can be taken as a measure of the nature of the catalytic site versus the number of contact points between these sites and the soot. A small difference indicates a very good contact between soot and catalyst; once the nucleus ignites, the oxidation process proceeds quickly. A large difference between T_{ign} and T_r indicates poor contact and once ignition takes place, depending on the nature of the site, the oxidation process proceeds rather slowly. This is very clear for the zirconia samples. Au promotes the formation of more-active sites, as can be seen in the difference in T_{ign} between the VZ and the VAZ samples (Table 5), in spite of a lower T_r or a lower reaction rate R for the proceeding oxidation due to the lack of contact points. For the VT samples one sees from T_{ign} again the presence of very active sites but use of higher amounts of vanadia seems to enhance the oxidation process (T_r) due to the presence of more contact points. The presence of gold particles diminishes the number of contact points and retards the oxidation process; i.e., there is a larger difference between T_{ign} and T_r when high V loadings are applied.

The results from this study indicate that Au–V catalysts are able to lower soot combustion parameters to the desired temperatures. Applying this system on an appropriate filter material makes it a promising system for soot control for diesel engines, although more investigation should be done, such as what the influence is of Au on the structure of the V compounds. Since it is unlikely this influence occurs during impregnation and aging of the catalysts one should focus on the calcination process. Together with a more extended spectroscopic analysis one should gain a clearer view of the relation between composition of the catalyst and its activity toward soot combustion. The mobility of catalytic systems guarantees the necessary contact between catalyst and soot. Generally catalysts with high mobility properties are very volatile. Therefore the durability of the catalyst should be studied in detail.

4. CONCLUSION

Vanadia-based catalysts are able to enhance the oxidation process of diesel soot particles and shift the ignition to lower temperatures. This effect increases with vanadia loading. The resulting activity is a superposition of two catalytic properties. In the first place, there is the intrinsic catalytic activity of the site, which depends on the nature of the species. The intrinsic activity determines the ignition of the soot by lowering the activation energy. Second, there is the number of these sites in contact with the soot together with the "wetting" capacity of the species. This property is important in solid–solid reactions, determines the further oxidation process, and is often a rate-determining factor. Monovanadyls might be the most active species but V_2O_5 crystallites provide a higher activity due to a better contact.

The addition of Au produces two effects. Au particles promote the oxygen transfer which increases the activity in the combustion of soot particles. This effect is clear at low V loadings when no V_2O_5 is present. According to Raman this same oxygen donor property might be also responsible for the formation of polyvanadate clusters instead of V_2O_5 crystallites, diminishing the mobility of the catalyst. This results in a decrease in activity because of the lack of contact points between soot and catalyst. This occurs at V loadings above saturation of the surface when V_2O_5 is present. Au particles do provide very active sites able to ignite the soot within the desired temperature range but retard the oxidation process at high V loadings because of the diminished contact.

ACKNOWLEDGMENTS

F. V. is indebted to the FWO Flanders (Fonds voor Wetenschappelijk Onderzoek—Vlaanderen) for financial support. This research has been performed in the frame of a D15 cost fund. We thank Texaco Technology Ghent for the generous gift of heavy-duty soot.

REFERENCES

1. Clunies-Ross, C., More, B. R., and Millar, G. J., *Nature* **381**, 379 (1996).
2. Barfknecht, T. R., *Prog. Energy. Comb. Sci.* **9**, 199 (1983).
3. Neeft, J. P. A., Ph.D thesis. Technical University of Delft, Delft, 1995.
4. http://www.dieselnet.com.
5. Farrauto, R. J., and Wedding, B., *J. Catal.* **33**, 249 (1973).
6. Iwamoto, M., Yahiro, H., Shundo, S., Yu-u, Y., and Mizuno, N., *Appl. Catal.* **69**, L15 (1991).
7. Zelenka, P., Cartellieri, W., and Herzog, P., *Appl. Catal. B* **10**, 3 (1996).
8. Whitehurst, D. D., Isoda, T., and Mochida, I., *Adv. Catal.* **42**, 345 (1998).
9. Armor, J. N., *Catal. Today* **38**, 163 (1997).
10. Dettling, J. C., and Skomoroski, R., U.S. Patent 5,100,632 (1992).
11. Homeier, E. H., and Joy, G. C., U.S. Patent 4,759,918 (1988).
12. Hartwig, M. M., U.S. Patent 4,510,265 (1985).
13. Alhström, A. F., and Odenbrand, C. U. I., *Appl. Catal.* **60**, 157 (1990).
14. Mul, G., Neeft, J. P. A., Kapteijn, F., Makkee, M., and Moulijn, J. A., *Appl. Catal. B* **6**, 339 (1995).
15. Neeft, J. P. A., Makkee, M., and Moulijn, J. A., *Appl. Catal. B* **8**, 57 (1996).
16. Neri, G., Bonaccorsi, L., Dato, A., Milone, C., Musolino, M. G., and Visco, A. M., *Appl. Catal. B* **11**, 217 (1997).
17. Badini, C., Saracco, G., and Serra, V., *Appl. Catal. B* **11**, 307 (1997).
18. Querini, C. A., Ulla, M. A., Requejo, F., Soria, J., Sedrán, U. A., and Miró, E. E., *Appl. Catal. B* **15**, 5 (1998)V.
19. Badini, C., Saracco, G., Serra, V., and Specchia, V., *Appl. Catal. B* **18**, 137 (1998).
20. Haruta, M., Tsubota, S., Kobayashi, T., Kageyama, H., Genet, M., and Delmon, B., *J. Catal.* **144**, 175 (1993).
21. Dekkers, M. A. P., Lippits, M. J., and Nieuwenhuys, B. E., *Catal. Today* **54**, 381 (1999).
22. Grisel, R. J. N., and Nieuwenhuys, B. E., *Catal. Today* **64**, 69 (2000).
23. Andreeva, D., Tabakova, T., Naydrenov, A., and Verpoort, F., *in* "Proceedings, 9th International Symposium on Heterogeneous Catalysis,

Varna (Bulgaria)," C21, p. 731. Marin Drinov Academic Publishing House, Sofia, Bulgaria, 2000.
23a. Andreeva, D., Tabakova, T., Ilieva, L., Naydrenov, A., Mehandjiev, D., and Abrashev, M., *Appl. Catal. A* **209**, 291 (2001).
24. Andreeva, D., Idakiev, V., Tabakova, T., and Andreev, A., *J. Catal.* **158**, 354 (1996).
25. Andreeva, D., Idakiev, V., Tabakova, T., and Giovanoli, R., *Bulg. Chem. Commun.* **30**, 59 (1998).
26. Ueda, A., and Haruta, M., *Appl. Catal. B* **18**, 115 (1998).
27. Went, G. T., Leu, L.-J., and Bell, A. T., *J. Catal.* **134**, 479 (1992).
28. Cristiani, C., Forzatti, P., and Busca, G., *J. Catal.* **116**, 586 (1989).
29. Haber, J., Kozlowska, A., and Kozlowski, R., *J. Catal.* **102**, 52 (1986).
30. Liu, Z. X., Xie, K., Li, Y. Q., and Bao, Q. X., *J. Catal.* **119**, 249 (1989).
31. Wachs, I. E., Briand, L. E., Jehng, J.-M., Burcham, L., and Gao, X., *Catal. Today* **57**, 323 (2000).
32. Khodakov, A., Olthof, B., Bell, A., and Iglesia, E., *J. Catal.* **181**, 839 (1999).
33. Neeft, J. P. A., van Pruisen, O. P., Makkee, M., and Moulijn, J. A., *Appl. Catal. B* **12**, 21 (1997).
34. Jelles, S. J., van Setten, B. A. A. L., Makkee, M., and Moulijn, J. A., *Appl. Catal. B* **21**, 35 (1999).
35. van Setten, B. A. A. L., van Dijk, R., Jelles, S. J., Makkee, M., and Moulijn, J. A., *Appl. Catal. B* **21**, 51 (1999).
36. Andrews, L., and Smardzewski, R., *J. Chem. Phys.* **58**, 2258 (1973).
37. van Doorn, J., Varloud, J., Mériaudeau, P., Perrichon, V., Chevrier, M., and Gauthier, C., *Appl. Catal. B* **1**, 117 (1992).